ELSEVIER

Journal of Biomechanics 31 (1998) 571–577

JOURNAL OF BIOMECHANICS

Technical Note

A high-accuracy three-dimensional coordinate digitizing system for reconstructing the geometry of diarthrodial joints

T.L. Haut[a], M.L. Hull[a,*], S.M. Howell[a,b]

[a]*Department of Mechanical Engineering, University of California, Davis, CA 95616, U.S.A.*
[b]*Clinical Investigation Facility, David Grant Medical Center, Travis Air Force Base, CA, U.S.A.*

Received 1 March 1997; received in revised form 24 November 1997

Abstract

This paper describes the design and performance evaluation of a three-dimensional (3-D) coordinate digitizing system (3-DCDS) for measuring both soft and hard biological tissue. The system incorporates a visible semiconducting laser beam and an X–Y positioning table to directly measure 3-D coordinates that define surface points. Experiments conducted to evaluate the performance of the system showed that it delivers an accuracy of 0.1 μm in the Z-direction and 1.4 μm in the X–Y plane, and an overall system root-mean-squared error (RMSE) of 8 μm on surfaces with slopes of less than 45°. This error is lower than that of previously reported measurement techniques. The 3-DCDS measures 3-D coordinates of surface points uniformly separated by 500 μm in the X–Y plane. Because the 3-DCDS is automated, the coordinates are measured efficiently and the accuracy is independent of operator skill. These highly accurate coordinates can be easily incorporated into nodal values for 3-D finite element models (FEM) of diarthrodial joints. To show the use of the 3-DCDS, the 3-D surface coordinates of human menisci were measured from a cadaver specimen.

Keywords: Three dimensional; Surface; Joints; Laser; Digitizing

1. Introduction

Finite element modeling (FEM) in orthopedic biomechanics requires a measurement technique to obtain accurate, three-dimensional (3-D) representations of diarthrodial joints (Mow et al., 1980; Spilker and Maxian, 1990). Accurate representations of joints, including soft tissue, articular cartilage, and bone, are needed for FEM to be useful in the study of joint behavior and orthopedic implants.

To accurately represent the articular surface of the human knee, an error of no more than 1% of the thinnest tissue is needed. Considering that the thickness of the articular cartilage is about 2 mm, a relative error of 1% would require an absolute error of 20 μm.

The absolute error of most currently available methods is much greater than 20 μm. The accuracy of thin-sectioning, photographing, and digitizing soft tissues is only 500 μm (McLeod et al., 1977; Meachim et al., 1977). The use of magnetic resonance imaging (MRI) (Cohen et al., 1997; Moon et al., 1983) and computed axial tomography (CT) to acquire tissue images also has an accuracy of 500 μm (Belsole et al., 1988; Garg and Walker, 1990). Stereophotogrammetry (SPG) the most accurate method for acquiring joint geometry, has an accuracy of 90 μm (Ateshian et al., 1991; Ghosh, 1983; Huiskes et al., 1985) which can be improved to about 20 μm using a digital camera placed at multiple stations (Ronsky et al., 1997).

The discriminating skill of the operator and the complexity of the measurement process are the principle reasons that these methods lose accuracy. For the methods that involve digitizing either photographs or images, the digitizing process is relatively imprecise. Although SPG is more accurate than these methods, the setup of the SPG system is complex. There are many sources of error, such as lens and photographic paper distortion, that can be introduced when using an optical measurement technique (Ateshian et al., 1991).

Considering the limitations of the previous methods, the goal of this study was the design of a new method for

*Corresponding author. Tel.: 001 530 752 6220; fax: 001 530 752 4158; e-mail: mlhull@ucdavis.edu.

0021-9290/98/$19.00
PII S0021-9290(98)00049-9

measuring diarthrodial joint geometry. The method had to meet the following criteria: (1) measure 3-D coordinates of surface points uniformly separated by 500 μm with an accuracy of at least 20 μm and (2) gain the desired performance independent of the operator's skill with efficiency. The subsequent sections describe the design of the system, accuracy evaluation, and application of the system to determine the geometry of the medial and lateral menisci in a human knee.

2. Materials and Methods

2.1. Design of 3-DCDS

To obtain 3-D coordinates that describe and represent the joint surfaces, the measurement system incorporates a semiconducting laser-based displacement sensor that works off triangulation to obtain the Z-coordinate of a point on the surface under the laser beam, in conjunction with an X–Y positioning table. This non-contacting 3-DCDS is modeled after a similar system described by Bhat et al. (1995). They used a laser-based measurement system for measuring changes in volume and surface area of a wound during healing.

The laser is mounted to a vertical cross-bar that can be translated in the Z-direction (Fig. 1). This commercially available, relatively inexpensive laser (LB1101, Keyence Corp., Woodcliff Lake, NJ) emits a visible red semiconducting, 670 nm wavelength beam that is converged to a 0.5 mm diameter point on the object. This beam is then scattered off the target and detected by the sensor head adjacent to the laser source. The laser works at a reference distance of 80 mm with a measuring range of $\pm$ 15 mm. The laser output is connected to an Analog Sensor Controller (RV3-35N, Keyence Corp., Woodcliff Lake, NJ), which processes analog output signals from the laser displacement sensor.

A linear X–Y positioning table (102004P, Parker Hannafin Corp., Daedal Division, Harrison, PA) houses the mounting fixture for the specimen. Low-noise (LN) electromagnetic microstepping motors with switch selectable motor/drive resolutions up to 101,600 steps rev^{-1} are driven by a controller to position the X and Y directions.

The controller for the drive motors and the output from the laser are monitored and controlled by an IBM-compatible PC with two serial ports. A Visual Basic (Microsoft Corp., Redmond, WA) program positions the table in the X–Y directions and reads the Z-coordinate from the laser. The output file created is a direct 3-D representation of the surface (X, Y, Z coordinates).

Mounted on top of the positioning table is a custom built fixture that holds specimens at the optimal reference distance from the laser sensor head. The housing allows for a specimen to be mounted in a circular tube, which rests in a square holding block. This allows for rotation in either the Y–Z or X–Z plane to $\pm$ 90°. These rotations allow surfaces with steep gradients to be measured by the laser system.

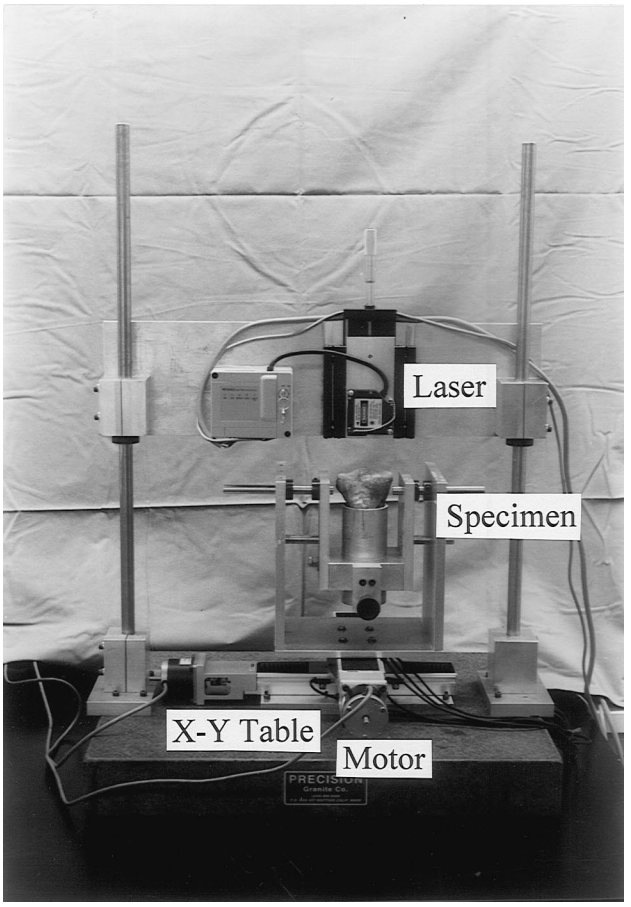

Fig. 1. Micrograph of the three-dimensional non-contacting coordinate digitising system. The human knee is mounted in the fixture below the laser and is positioned so that the superior articulating surface is facing the lasser. The motors systematically move the X–Y table to allow the laser to scan over the entire surface of the meniscus.

2.2. Accuracy evaluation of the system

The accuracy and precision of the laser's displacement sensor was verified by comparing gage blocks of a known height with the measurements obtained by the laser. The heights of the gage blocks were 2542.5, 2562.9, and 5080.0 $\pm$ 2.5 μm. The difference between the true value and the measured value was calculated to be the error. Similarly, the X–Y positioning table accuracy and precision were verified by moving each axis a defined distance. The true distance was then measured by a laser interferometer. Again, the difference between how far the table actually moved and the defined input distance was calculated to be the error. For both the laser and the table, the mean and the standard deviation of the error gave the accuracy and precision, respectively.

The fixture was tested to determine whether it introduced any error into the measurement. A single X,Y point on a gage block was measured by the laser, and then the fixture was rotated throughout its entire range of motion. The fixture was returned back to the original location and the laser measurement taken again. The average and the standard deviation of the laser's measurement was calculated. Since the positioning table was fixed during these repeated measurements, the precision of this measurement was only a combination of the laser and the rotation of the fixture. Since both the laser and the rotation of the fixture are random variables and the precision of the laser was known from an earlier calculation, the precision of the fixture alone was calculated.

The overall system error was calculated for various slopes by transforming the error in the X–Y positioning into the Z-direction and then adding the Z-direction error. To make this transformation, each of the measurement errors was treated as an independent random variable with a Gaussian distribution and the algebra of normal functions was used to compute the apparent error in the Z-direction due to the error contributions from both the laser and the X–Y positioning table. (See Appendix).

Additionally, using two random points on a human meniscus and two random points on a human tibial plateau, the system precision was evaluated. This was performed by repeatedly moving the table to these four points and taking six repeated measurements. This was performed while the table was stationary and with the table moving. The standard deviations were computed for both the static and the dynamic test at all four points.

2.3. Determination of the geometry of the menisci

The biomechanical applicability of the 3-DCDS was demonstrated by reproducing the geometry of the medial and lateral menisci of the human knee. One fresh-frozen cadaveric knee was thawed at room temperature. The knee was disarticulated and soft tissue was removed leaving just the medial and lateral meniscus attached to the tibial plateau. After potting the diaphysis of the tibia in the circular tube held by the testing fixture, the articular surface was scanned. A grid resolution of 0.5 mm by 0.5 mm was applied to the 80 mm × 60 mm articular surface of the tibia resulting in 19,200 data points. Scanning both menisci and the adjoining articular surface required 25 min. The anterior, posterior, medial and lateral edges of the menisci were then measured by rotating and scanning the specimen with the respective edges facing the laser. The menisci were removed and the exposed tibial plateau was then scanned by the laser. The six scans provided data for the complete characterization of the geometry of both the medial and lateral menisci. The X,Y,Z data were then transformed back into the original reference frame that the articular surface was scanned in. A finite element package (PATRAN, MacNeal-Schwendler Corp., Los Angeles, CA) was used to visualize the menisci in 3-D.

3. Results

The laser had an accuracy of 0.1 μm and a precision of 2.4 μm (Table 1). The accuracy of the X–Y positioning table was 1.4 and 0.4 μm in the X and Y directions, respectively. The precision of each individual component of the system was better than 3.5 μm.

Combining the errors of all of the components through the use of algebra of normal functions gave an overall system accuracy and precision which depended on the slope (Table 2). As the slope increased, there was a loss in both accuracy and precision.

The precision of the system at the two random menisci points with the table stationary was 3 and 2 μm. With the table moving these standard deviations increased to 6 and 10 μm, respectively. The precision for the two random tibial plateau points during a stationary test was 1 μm for both the points. Again, this imprecision increased to 2 and 6 μm during the dynamic test.

The finite element package enabled a clear view of the 3-D coordinates representing the surfaces of the menisci (Fig. 2). A 10 μm or less difference in the Z-coordinate between the scans with and without the menisci was assumed to represent the boundary of the menisci.

4. Discussion

The laser measurement system meets the criteria necessary to obtain an accurate geometric representation of diarthrodial joints. This system is non-contacting which

Table 1
Accuracy and precision of the laser and X–Y positioning table

	Laser (μm) $n=6$	X-direction (μm) $n=9$	Y-direction (μm) $n=9$
Error	+ 1.5	0.0	0.0
Error	− 1.5	+ 3.5	+ 2.2
Error	+ 2.1	+ 5.3	+ 3.3
Error	− 3.9	+ 3.4	+ 1.9
Error	+ 2.0	+ 4.6	+ 2.2
Error	− 1.0	+ 0.3	− 0.3
Error		+ 2.4	− 1.7
Error		− 3.7	− 4.8
Error		− 3.2	− 6.4
Mean (accuracy)	− 0.13	1.4	− 0.4
st. dev. (precision)	2.4	3.3	3.4

Table 2
Overall system accuracy and precision

	Accuracy (μm)	Precision (μm)
30°	2.5	6.0
45°	4.3	7.2
60°	7.4	9.1
75°	15.7	14.5

is important when dealing with soft tissues that can deform easily even if small amounts of pressure are applied (Ronsky et al., 1997). The results from overall error analysis indicate that as the slope increases, so does the error (Table 2). However, the fixture allows for rotation of the specimen so that surfaces with steep gradients can be rotated into a plane beneath the laser to reduce slopes to less than 45°. In our example of the human menisci, the steep slopes of anterior, posterior, medial and lateral edges were too large to measure accurately with the superior articular surface facing the laser. To correct for this, each edge was rotated so that it was in a plane beneath the laser and was easily measured without the presence of large slopes. Because the maximum slope is bound by 45°, the worst values of accuracy and precision are 4 and 7 μm, respectively, giving a root-mean-squared error (RMSE) of 8 μm. Thus the geometric data for a human cadaveric knee obtained by this new system are more accurate than the previously reported techniques (Ateshian et al., 1991; Belsole et al., 1988; Cohen et al., 1997; McLeod et al., 1977) including digital photogrammetry which has an RMSE value of 19 μm for the Z-coordinate (Ronsky et al., 1997).

The current grid size resolution, 0.5 mm, is the smallest of all methods used for obtaining geometric data. This grid size limits the resolution in the X–Y plane and therefore an accurate edge detection may be difficult. Due to the spot diameter of the laser and time constraints on scan time, this is the smallest grid size that was practical. In contrast to SPG where the grid size can vary from 0.7 to 2.3 mm depending on the curvature of the surface (Ateshian et al, 1991), the grid size is constant over the entire scan area. The current system's grid size is small compared with MRI, CT and sliced photographs where the slice thickness is generally 3 mm. However, a recent study shows MRI slices as thin as 1 mm (Cohen et al., 1997).

In addition to being highly accurate, the 3-DCDS is simple to construct and operate. The entire system has only four main components which include the laser with controller, the positioning table with the drive motors and controller, the PC to coordinate the two above components, and the mounting fixture. Calibration and reference markers are not needed for the current system, as they are in the other methods described. The system can easily be rotated to allow for scanning in other orthogonal planes and hence, increase the scanning area. Unlike SPG, where multiple photographs have to be taken and additional corresponding realignments performed to relate information from one region to the other

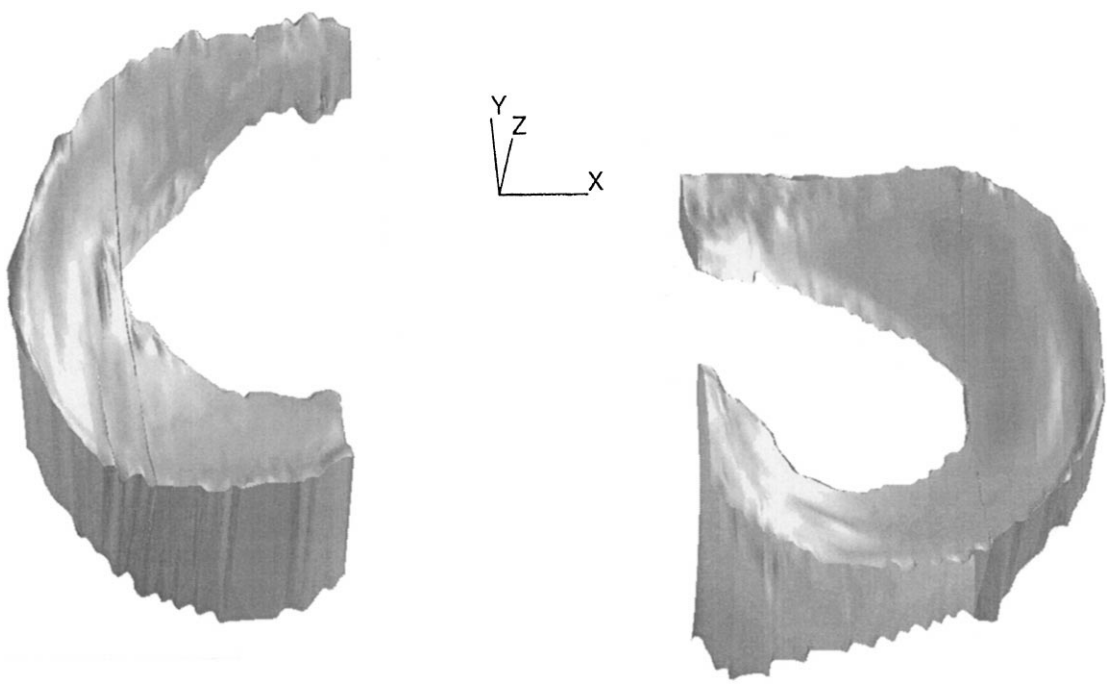

Fig. 2. Three-dimensional representation of medial and lateral meniscus of a right knee viewed from the posterior aspect. The coordinate system directions are X — lateral, Y — anterior, and Z — superior. The lines are introduced by the solid modeling software.

(Huiskes et al., 1985), the transformation resulting from our rotation is simple based on the center and angle of rotation. Other than rotating the specimen manually, the system is fully automated so that the results are achieved efficiently and their quality does not depend on the skill of the operator.

Although the example explained the use of the system in quantifying the geometry of the meniscus, FEM models that investigate contact in diarthrodial joints require both cartilage and possibly bone. The system can be used to accurately measure cartilage thickness and bone surface geometry. To measure the cartilage thickness, a scan of the articulating cartilage surface would be performed using the 3-DCDS. Then the specimen would be submerged in a solution of 5.25% sodium hypochlorite to dissolve the cartilage layer down to the level of the tidemark (Ateshian et al., 1991). The specimen would be scanned a second time with the cartilage removed to obtain thickness measurements. This second scan would also give the bone surface geometry. Because the measurement with the laser is not affected by either surface texture, translucency, or colors, the error in the measurement of all of these tissues would be consistent and comparable with that reported here. Thus, contrast coating of bone surfaces is not necessary as it is in SPG, where it is required to improve grid contrast (Ateshian et al., 1991). If the thickness of the cortical shell was also of interest, then an additional measurement technique that gives images of slices through the bone would be required.

One source of error inherent to all measurement techniques that expose the joint surfaces to air is dehydration of the tissues during the measurement process. Because soft tissues contain approximately 60–70% water, dehydration may occur to some extent during the 25 min period required to image the meniscus which would affect the volume of the tissue. However, this effect is complex to quantify because dimensional changes of the meniscus, articular cartilage, and/or bone may give rise to changes in the measurement obtained with the laser. Lacking a method of ascribing dimensional changes to the individual tissues, the dimensional changes due to meniscus dehydration per se cannot be distinguished. This is an area that merits further investigation.

Acknowledgements

The authors are grateful to the United States Air Force (SGO #96177) and the Mercy Medical Foundation for their financial support.

Appendix

To calculate the overall system accuracy for the 3-DCDS, the inaccuracies in the X and Y directions must be referred into the Z-direction. This was accomplished by starting with a certain point on a surface that is to be measured. The inaccuracy in positioning the X–Y table will locate a different point on the surface. If this surface is parallel to the X–Y plane, then there will be no resulting apparent change in the Z-direction with an inaccurate positioning of the table. However, if this surface is sloped, then this inaccuracy in the positioning table will become apparent in the Z-direction.

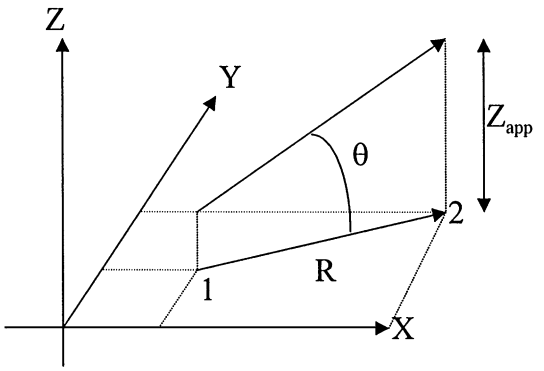

Fig. 3. Errors in positioning in the X–Y plane manifest as errors in the Z-direction if the surface to be mesured is sloped.

To explain how errors in the X and Y directions manifest as errors in the Z-direction, consider two points on the X–Y plane, point 1 and point 2 (Fig. 3). Assume the table was to position at point 1 but instead went to point 2. The radius R can be computed from point 1 to point 2. Then, if the surface of interest is sloped, a change in the Z-direction will become apparent between point 1 and point 2. Denoted as Z_{app}, this change in Z becomes $Z_{app} = R \tan\theta$ where θ is the slope. By assuming that the errors in all coordinate directions are normally distributed and independent random variables, the accuracies, and precisions in all three directions can be computed to one total apparent accuracy and precision in the Z-direction.

In developing the mathematical details of the procedure, the three independent normally distributed variables are x, y and z. Th accuracy μ and the precision σ for each variable are known. Additionally, the precision of the fixture is known.

variable $x = X$-direction positioning table μ_x, σ_x,

variable $y = Y$-direction positioning table μ_x, σ_y,

variable $z = Z$-direction laser μ_z, σ_z,

variable fix = fixture precision, σ_{fix}.

If the radius R from point 1 to point 2 is computed as

$$R = (x^2 + y^2)^{1/2}, \tag{A.1}$$

then the accuracy and precision for both x^2 and y^2 must first be computed. For binary operations on normally

distributed random variables, the distribution parameters become (Haugen, 1968)

$$\mu_{xx} = \mu_x^2 + \sigma_x^2, \qquad \mu_{yy} = \mu_y^2 + \sigma_y^2, \tag{A.2}$$

$$\sigma_{xx} = [4\mu_x^2\sigma_x^2 + 2\sigma_x^4]^{1/2}, \qquad \sigma_{yy} = [4\mu_y^2\sigma_y^2 + 2\sigma_y^4]^{1/2}. \tag{A.3}$$

An intermediate random variable g is computed as

$$g = x^2 + y^2. \tag{A.4}$$

Assuming that x and y are independent, the accuracy and precision for g becomes

$$\mu_g = \mu_{xx} + \mu_{yy}, \tag{A.5}$$

$$\sigma_g = [\sigma_{xx}^2 + \sigma_{yy}^2]^{1/2}. \tag{A.6}$$

Noting that

$$R = (g)^{1/2}, \tag{A.7}$$

the distribution parameters for the square root of a normal function are

$$\mu_R = \{1/2[4\mu_g^2 - 2\sigma_g^2]^{1/2}\}^{1/2}, \tag{A.8}$$

$$\sigma_R = \{\mu_g - 1/2\,[4\mu_g^2 - 2\sigma_g^2]^{1/2}\}^{1/2}. \tag{A.9}$$

Because $Z_{\text{app}} = R\tan(\theta)$

$$\mu_{z_{\text{app}}} = \mu_R \tan(\theta), \tag{A.10}$$

$$\sigma_{z_{\text{app}}} = \sigma_R \tan(\theta). \tag{A.11}$$

Then, by adding the apparent Z to the both the actual Z and the fixture, the total accuracy and precision are calculated as

$$\mu_{z_{\text{tot}}} = \mu_z + \mu_{z_{\text{app}}}, \tag{A.12}$$

$$\sigma_{z_{\text{tot}}} = [\sigma_2^2 + \sigma_{z_{\text{app}}}^2 + \sigma_{\text{fix}}^2]^{1/2}. \tag{A.13}$$

As is evident from Eq. (A.11), both the accuracy and the precision of the total depend on the surface angle θ and a loss in accuracy and precision occurs with increasing slope of the surface.

A.1. Sample calculation

This sample calculation explains how the accuracy and precision values in Table 2 were obtained.

With units of microns, the accuracies and precisions of the individual components are

$\mu_x = 1.4, \qquad \sigma_x = 3.4,$

$\mu_y = 0.4, \qquad \sigma_y = 3.3,$

$\mu_z = 0.1, \qquad \sigma_z = 2.4,$

$\sigma_{\text{fix}} = 2.1,$

calculate

$\mu_{xx} = 13.5, \qquad \mu_{yy} = 11.1,$

$\sigma_{xx} = 18.9, \qquad \sigma_{yy} = 15.6,$

$g = x^2 + y^2$:

$\mu_g = 24.6, \qquad \sigma_g = 24.5,$

$R = (g)^{1/2}$:

$\mu_R = 4.2, \qquad \sigma_R = 2.7,$

Apparent $Z = R\tan(30)$:

$\mu_{z_{\text{app}}} = 2.4, \qquad \sigma_{z_{\text{app}}} = 1.5$

Total accuracy and precision

$$\mu_{z_{\text{tot}}} = \mu_z + \mu_{z_{\text{app}}} = 0.1 + 2.4 = 2.5,$$

$$\sigma_{z_{\text{tot}}} = \sigma_z + \sigma_{z_{\text{app}}} + \sigma_{\text{fix}} = 2.4 + 1.5 + 2.1 = 6.0$$

References

Ateshian, G.A., Soslowsky, L.J., Mow, V.C., 1991. Quantitation of articular surface topography and cartilage thickness in knee joints using stereophotogrammetry. Journal of Biomechanics 24, 761–76.

Belsole, R.J., Helbelink, D.R., Llewellyn, J.A., Stenzler, S., Green, T.L., Dale, M., 1988. Mathematical analysis of computed carpal models. Journal of Orthopaedic Research 5, 116–122.

Bhat, S.S., Smith, D.J., 1994. Liver and sound scanner for non-contact 3D volume measurement and surface texture analysis. Physiological Measurements 15, 79–88.

Cohen, Z.A., McCarthy, D.M., Ateshian, G.A., Kwak, S.D., Peterfy, C.G., Alderson, P., Grelsamer, R.P., Henry, J.H., Mow, V.C., 1997. In vivo and in vitro joint cartilage topography, thickness, and contact areas from MRI. Transactions of the Orthopedic Research Society 43, 625.

Feldkamp, L.A., Goldstein, S.A., Parfitt, A.M., Jesion, G., Kleerekoper, M., 1989. The direct examination of three-dimensional bone architecture in vitro by computed tomography. Journal of Bone and Mineral Research 4, 3–11.

Garg, A., Walker, P.S., 1990. Prediction of knee joint motion using a three-dimensional computer graphics model. Journal of Biomechanics 23, 45–58.

Ghosh, S.K., 1983. A close-range photogrammetric system for 3-D measurements and perspective diagramming in biomechanics. Journal of Biomechanics 16, 667–74.

Haugen, E.B., 1968. Chap. 3. Algebra of normal functions. In: Probabilistic Approaches to Design. Wiley, New York.

Huiskes, R., Kremers, J., de Lange, A., Woltring, H.J., Sevik, G., van Rens, T. J., 1985. Analytical stereophotogrammetric determination of three-dimensional knee joint geometry Journal of Biomechanics 18, 559–70.

McLeod, W.D., Moschi, A., Andrews, J.R., Hughston, J.C., 1977. Tibial plateau topography. American Journal of Sports Medicine 5, 13–18.

Meachim, G., Bentley, G., Baker R., 1977. Effect of age on thickness of adult patellar articular cartilage. Annals of Rheumatoid Disease 36, 563–568.

Moon, K.L., Genant, H.K., Davis, P.L., Chafetz, N.I., Helms, C.A., Morris, J.M., Rodrigo, J.J., Jergesen, H.E., Brasch, R.C., Bovill, E.G., 1983. Nuclear magnetic resonance imaging in orthopaedics: principles and applications. Journal of Orthopaedic Research 1, 101–114.

Mow, V.C., Kuei, S.C., Lai W.M., Armstrong, C.G., 1980. Biphasic creep and stress relaxation of articular cartilage: theory and experiment. Journal of Biomedical Engineering 102, 73–84.

Ronsky, J.L., Boyd, S.K., Lichti, D.D., Chapman, M.A., Salkauskas, K., 1997. Precise measurement of articular cartilage surfaces: comparison of multi-station digital photogrammetry with 3D digitization. Proceedings of the 1997 Bioengineering Conference, BED-vol. 35. American Society of Mechanical Engineers, New York, NY, pp. 39–40.

Spilker, R.L., Maxian, T.A., 1990. A mixed-penalty finite element formulation of the linear biphasic theory for soft tissue. International Journal of Numerical Methods in Engineering 30, 1063–1082.